D.J. Murray-Smith
Mathematical and Computer Modelling of Dynamical Systems

Inverse Simulation and Analysis of Underwater Vehicle Dynamics Using Feedback Principles

David J. Murray-Smith*

School of Engineering,
University of Glasgow,
Glasgow G12 8QQ,
Scotland,
United Kingdom.

*E-mail: david.murray-smith@glasgow.ac.uk

D.J. Murray-Smith
Mathematical and Computer Modelling of Dynamical Systems

Abstract

Inverse simulation is a technique used in the modelling of dynamic systems that allows time histories of input variables to be found that generate required model output responses and provide inverse solutions in cases where analytical approaches to model inversion can present difficulties. This paper describes the application of inverse simulation to a nonlinear dynamic model of an underwater vehicle (UUV) and the determination of vehicle control inputs for specified manoeuvres. The approach to inverse simulation used in this application is based on the principles of feedback. Design issues relating to the UUV control surfaces and propeller thrust are highlighted through this procedure. The paper includes an outline of the nonlinear model of the UUV and typical sets of experimental conditions. Feedback loops are designed around the model for selected output variables and the inverse solutions are generated through simulation of this multi-input multi-output closed-loop system. It is shown that the feedback approach can provide inverse solutions for an appropriate choice of loop gain factors and integration time step using a fixed-step integration algorithm. Inverse solutions generated in this way are shown provide insight concerning issues of vehicle handling and manoeuvrability in a more direct fashion than is possible using conventional simulation methods.

Keywords: Simulation, inverse, nonlinear, model, feedback, underwater vehicle, actuator, manoeuvre.

1. Introduction

Techniques based on inverse dynamic models allow time histories of input variables to be found that correspond to a given set of output time history requirements and are important for many dynamic problems, especially for investigation of actuator performance and limits. Applications in which inverse modelling has been recognised as particularly valuable include aircraft handling qualities investigations and agility studies, both for fixed-wing aircraft and for helicopters (see, e.g., [1], [2]). In such cases the inverse solution provides vital information about the relative difficulty of performing different manoeuvres, the inherent agility of the vehicle and the control margins available to the pilot as actuator amplitude or rate limits are approached.

In the nonlinear case the derivation of an analytically-based inverse model can present difficulties and, in recent years, increasing use has been made of simulation-based methods for the generation of inverse solutions. Several inverse simulation methods have been developed which have origins in aircraft handling qualities applications, as mentioned above, and a useful review of some techniques developed specifically for aeronautical applications has been provided by Thomson and Bradley [3]. The most widely used of these methods involves repeated solution of a conventional forward simulation model and the first published account of this type of approach was by Hess, Gao and Wang [1]. Similar 'integration based' methods have been developed by Thomson and Bradley and their colleagues (see e.g. [3]). These techniques, which are all iterative in nature, are based mainly on gradient methods, although search-based optimisation techniques have also been used successfully for a number of different applications (see, e.g. [4]). A second type of approach, which also has its origins in aircraft flight mechanics modelling and handling qualities studies, is the so-called 'differentiation method' in which the ordinary differential equations of the given model are transformed into finite difference equations. This approach was developed by Thomson and his colleagues at the University of Glasgow in the context of helicopter problems (see e.g. [5], [6]) and by Kato and Suguira [7] for fixed-wing aircraft applications. Methods that involve other forms of optimisation include techniques developed by Lee and Kim [8] and by Celi [9]. Rather different methods of inverse simulation have been developed in the context of automatic control and robotics applications. These include numerical approaches base on techniques involving the numerical solution of differential algebraic equations (see e.g. [10], [11]). More detailed accounts of these approaches to inverse simulation and discussion of the strengths and weaknesses of a number of different methods may be found elsewhere (e.g. [2], [3], [11]).

In addition, it should be noted that the theory of flat systems is also highly relevant for inverse simulation since a model that has the property of flatness allows all state variables and inputs to be expressed in terms of a "flat output" and a finite number of derivatives of that flat output (see e.g. [12]). This systems-theory concept has been linked, for the nonlinear case, to the ideas of controllability in linear systems theory and has direct relevance for the development of nonlinear inverse simulation models. Approaches to inverse modelling and simulation based on flatness have been applied by a number of other

researchers including a study in which a DAE formulation has been compared with a flatness-based approach for an application involving crane dynamics and control [13]. In the context of control applications based on internal model control (IMC) techniques, much use has been made of inverse models and in some cases implementations have involved inverse simulations based on artificial neural network methods (see e.g. [14]).

A completely different type of methodology for inverse simulation involves the use of feedback principles. Early developments took place at the German DLR aerospace research institute at Braunschweig and work relating to this is discussed in a report by Buchholz and von Grünhagen [15]. Quite separately, a similar type of approach, termed 'inverse dynamics compensation via simulation of feedback control systems' (IDCS) was developed in Japan by Tagawa and Fukui [16] who have applied the method to a variety of nonlinear problems. Use of the IDCS methodology for some specific applications, including servo-hydraulic actuators and robotics, is described in two recent papers [17], [18].

These feedback-based methods have origins which can be traced to the use of feedback principles for operations such as division and inverse function generation in electronic analog computers. Recent experience with the feedback approach has shown that it has wide applicability [11], [19] and is not restricted to the use of simple proportional feedback pathways involving simple gain factors. More complex forms of feedback structure can be applied successfully (see e.g. [11], [19]).

While choice of the feedback structures necessary for the feedback-based approach appears to introduce some additional complexity to the inverse simulation process, it should be noted that the development of an inverse simulation using this approach is much less challenging that the design of an equivalent feedback system for control. This is because issues of plant uncertainty and external disturbances are not relevant in the inverse simulation case (see e.g. [11], [19]). Also, the computational efficiency of the feedback approach (once the initial stage involving development of the feedback structure has been completed) is usually high compared with some of the iterative approaches outlined above which tend to be more numerically intensive. The feedback-based approach can be particularly useful for some problems involving hard nonlinearities, such as saturation effects, where difficulties associated with calculation of the Jacobian matrix mean that gradient-based iterative methods fail to converge and the use of computationally-expensive search-based optimisation algorithms has been proposed (see e.g. [4]).

The feedback-based approach adopted in this work also allows parameter sensitivity analysis methods to be used to analyse the dependence of inverse solutions on parameters of the forward model without the need for parameter perturbation techniques. This is achieved through the use of sensitivity models [20]. The sensitivity model approach can have advantages, especially in the linear case, in terms of the additional physical insight provided when compared with the parameter perturbation method.

2. Feedback methods for inverse simulation

The principles of inverse simulation based on the use of feedback properties can be illustrated using the block diagram of Fig. 1 for the case of a single-input single-output linear model $G(s)$ and a feedback loop involving a cascaded block with transfer function $K(s)$. For this simple feedback structure the transfer function relating the variable $W(s)$ to a reference input $V(s)$ is given by:

$$\frac{W(s)}{V(s)} = \frac{1}{\frac{1}{K(s)} + G(s)} \tag{1}$$

If the magnitude of the term $1/K(s)$ is very small compared with the magnitude of $G(s)$, over the range of frequencies of interest, the transfer function may be approximated by:

$$\frac{W(s)}{V(s)} \approx \frac{1}{G(s)} \tag{2}$$

Thus, if $K(s)$ is large, the transfer function $W(s)/V(s)$ is a close approximation to the inverse model. It should be noted that the values of gain constants that apply in any specific application depend on the units of the input and output variables of the model. In cases involving several feedback loops, any comparison of the gain constants used for different loops must take account of the units involved.

Although this discussion relates to a linear single-input single-output form of model, the same principles may be applied in the case of multi-input multi-output model structures and may also be used for nonlinear models. Simple proportional high-gain feedback provides acceptable solutions in many cases, but the approach is not limited to proportional control methods and the principles of feedback-based model inversion apply also to other feedback structures. The approach used in the application described in this paper builds upon methods which have been reported previously ([11], [19], [20]).

For an application in which a linearised form of model is available, classical analysis of the chosen feedback structure can be carried out using frequency domain or root locus methods. Parameters of the controller block can then be adjusted to try to ensure that poles of the inverse simulation model are located at points in the *s*-plane close to the positions of the zeros of the forward model. Any branches of the root locus that tend towards infinity in the *s*-plane as the gain factor becomes large can also be identified and their influence on the inverse simulation can be established.

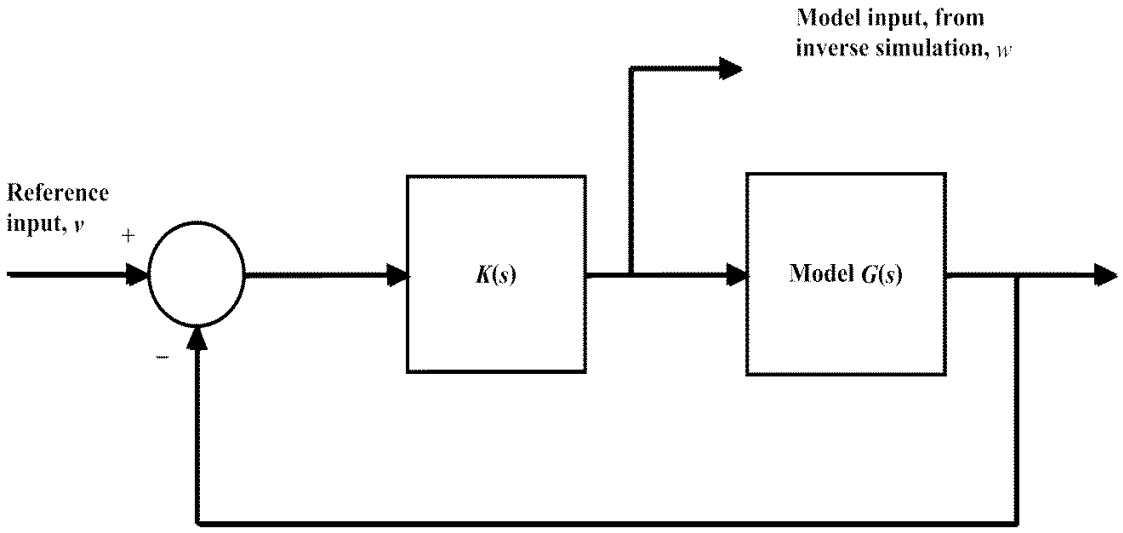

Fig.1. Block diagram showing the structure of the feedback system used for inversion of a given model *G*. The reference signal for the feedback system is the required output ***v***. For a high gain ***K*,** the variable *w* obtained from simulation of this feedback system approximates the model input that would be required to produce an output closely matching the reference signal *v*.

3. The underwater vehicle model

The underwater vehicle model considered in this study was developed by Healey and Lienard [21] to describe a specific unmanned underwater vehicle, the NPS AUV II. This UUV model has been modified by McGookin, as described by Zenor, Murray-Smith, McGookin and Crosbie [22].

3.1 The basic six-degrees-of-freedom model.

The model is nonlinear in structure and, applying widely-used notation [23], the general body-fixed vector representation has the form:

$$\mathbf{M}\dot{\upsilon} + \mathbf{C}(\upsilon)\upsilon + \mathbf{D}(\upsilon)\upsilon + \mathbf{g}(\boldsymbol{\eta}) = \boldsymbol{\tau} \tag{3}$$

$$\dot{\boldsymbol{\eta}} = \mathbf{J}(\boldsymbol{\eta})\upsilon \tag{4}$$

Here the matrix $\mathbf{M}$ is the inertia matrix (which includes added mass effects); the matrix $\mathbf{C}(\upsilon)$ is the matrix of Coriolis and centripetal terms and also includes added mass effects; the matrix $\mathbf{D}(\upsilon)$ is the damping matrix; the vector $\mathbf{g}(\boldsymbol{\eta})$ is the vector of gravitational forces and moments; and $\boldsymbol{\tau}$ is the vector of external forces and moments. The matrix $\mathbf{J}(\boldsymbol{\eta})$ is a transformation matrix which relates the body-fixed and earth-fixed coordinate systems.

Interpretation of (3) and (4) is based on standard conventions used in the modelling of underwater vehicles. The body-fixed frame involves the six translational and rotational velocities, as defined conventionally for marine vehicle models by the vector $\boldsymbol{\upsilon}(t) = [u(t), v(t), w(t), p(t), q(t), r(t)]^T$ relative to a constant velocity coordinate frame moving with the ocean current which has a velocity vector $\boldsymbol{u_c}$ (see, e.g., [23]). In this representation $u(t)$ is the surge velocity, $v(t)$ is the sway velocity, $w(t)$ is the heave velocity, $p(t)$ is the roll rate, $q(t)$ is the pitch rate and $r(t)$ is the yaw rate. The six components of the global reference frame are given by the vector $\boldsymbol{\eta}(t) = [x(t), y(t), z(t), \phi(t), \theta(t), \psi(t)]^T$ where $x(t)$, $y(t)$ and $z(t)$ define the position of the centre of mass of the vehicle and the angles $\phi(t)$, $\theta(t)$ and $\psi(t)$ are related through standard Euler transformations to the body roll angle, pitch angle and yaw angle (heading) variables. The external forces and moments given by the vector $\boldsymbol{\tau}$ involve gravitational, buoyancy, hydrodynamic and propulsive components. Control surface deflections of the rudder, $(\delta_r(t))$, port bow plane $(\delta_{bp}(t))$, starboard bow plane $(\delta_{bs}(t))$ and the stern plane $(\delta_s(t))$, provide forces and moments for control of the vehicle together with inputs arising from the propeller rotational rate $(n(t))$ and buoyancy adjustment $(B(t))$.

A set of six nonlinear equations for surge, sway, heave, roll, pitch and yaw motion can be derived from this representation. Parameters used are as given in [21] but the parameter list had to be extended to include changes made to the representation of the propeller, as discussed in Section 3.2. Time constants for the control surfaces and associated actuators are considered to be negligible compared with the dynamics of the vehicle.

The model of the UUV may be converted into standard state-space form by rearranging (3) and (4) to give the following equation:

$$\begin{bmatrix} \dot{\boldsymbol{\eta}} \\ \dot{\boldsymbol{\upsilon}} \end{bmatrix} = \begin{bmatrix} \mathbf{J}(\boldsymbol{\eta})\boldsymbol{\upsilon} \\ \mathbf{M}^{-1}\{-(\mathbf{C}(\boldsymbol{\upsilon}) - \mathbf{D}(\boldsymbol{\upsilon}))\boldsymbol{\upsilon} - \mathbf{g}(\boldsymbol{\eta}) + \boldsymbol{\tau}\} \end{bmatrix} \tag{5}$$

which has the general nonlinear matrix-vector form:

$$\dot{\mathbf{x}} = \mathbf{F}(\mathbf{x}, \mathbf{u}) \tag{6}$$

where $\mathbf{x}$ is the state vector and $\mathbf{u}$ is the control input vector.

3.2 Modelling of the propellers and associated shaft load

Some relatively minor changes were found to be necessary in the model presented by Healey and Lienard [21] in order to make the simulation model perform in a credible way over a wider range of operating conditions for a real-time simulation application [22]. Changes were also needed to allow more detailed consideration of the performance in complex manoeuvres.

The model changes included modifications to the equations representing the propeller in order to allow the model to function correctly as the propeller speed dropped to zero. The changes also ensured that an undesirable situation involving a divide-by-zero condition that could occur with the original representation with zero initial propeller speed was eliminated.

The main change involved replacing the thrust equation within the existing model. First it was assumed that the UUV produces a single propulsive force, although it has two propellers. The resulting thrust produced by the equivalent single propeller is calculated from the *Bilinear Thruster Model* [23] as:

$$T = T_{nn}|n|n + T_{nu}|n|u \tag{7}$$

The quantity n is the rotational speed of the propeller and the values for the coefficients T_{nn} and T_{nu} are given [23] by:

$$T_{nn} = \rho D^4 \alpha_1 \tag{8}$$

$$T_{nu} = \rho D^3 \alpha_2 \tag{9}$$

$$\alpha_1 = 0.12 - 0.5\alpha_2 \tag{10}$$

In these expressions the parameter D represents the diameter of the propellers, which is given as 30 cm. For the surge velocity profile for the NPS AUV II the value for α_2 is chosen to be -0.16, which gives a value for α_1 of 0.019. Combining Equations (7) to (10) gives the ideal total propeller thrust. However, the propeller does not have perfect efficiency and the surge force produced by the propulsion system for a value of 70% efficiency (which is regarded as reasonable for this application) is given by:

$$X_{prop} = 0.7T \tag{11}$$

It should be noted that only the surge velocity equation is involved since the propellers only produce thrust in the direction of the longitudinal axis. It should also be noted that rotational effects of the propellers in roll and yaw are taken to be negligible since the propellers operate together in a counter-balancing manner.

As well as representing the propeller thrust, the model has to incorporate an element to represent the load on the drive shaft due to rotation of the propeller in the water. This involves approximating the propeller by a rotating disc and must take account of the various moments acting on the propeller.

The input is the torque applied by the shaft, T_{SHAFT}, which is the torque needed to make the propeller balance the drag and inertia components. The equation of motion for the propeller can be shown to have the form [22]:

$$T_{SHAFT} = I_o \dot{n} + \frac{1}{2}\rho C_D n^2 R_{DISC}{}^3 \tag{15}$$

where R_{DISC} is the radius of the rotating disc in the approximation mentioned above, the parameter C_D is an associated drag coefficient, ρ is the density of water and n is the rotational speed of the propeller. It follows that the load moment on the propeller, T_{LOAD}, is given by the equation:

$$T_{LOAD} = -T_{SHAFT} = -I_o \dot{n} - \frac{1}{2}\rho C_D n^2 R_{DISC}{}^3 \tag{16}$$

This representation gives the approximate load on the shaft and, within this expression, the only parameter that is not readily available is the drag coefficient, C_D , However, a disc rotating about its longitudinal axis is known to have a drag coefficient of 1.369×10^{-3} [24] and this approximate value has therefore been applied [22]. In this representation no account is taken of added mass and of the dynamics of the shaft itself.

4. Inverse simulation of the nonlinear model for required output responses of simple form

The nonlinear state-space simulation model applied in this investigation has involved a modified version of a MATLAB model developed by Fossen and his colleagues, which is available on-line as part of the Marine Systems Simulator software set [25]. The simulation model allows for limits on each of the six input variables and has been modified to include the changes detailed in Sections 3.1 and 3.2. The modified version of the simulation program includes a separate function that returns the motor load torque from the propeller load. The main program allows testing of the simulation model for any set of initial conditions in terms of the system state and any prescribed pattern of input activity at the actuators. Within this routine the user can set the integration step size, communication interval and end time for the simulation. For the cases considered here a fixed-step Runge-Kutta integration method has been used with an integration step time of 0.01 s and communication interval of 0.1 s.

The first, relatively simple, illustrations of the use of the feedback approach to inverse simulation for the nonlinear UUV model involve forward diving motion and lateral directional motion to determine the propeller, stern-plane and rudder input time histories required to achieve desired patterns of surge velocity, pitch rate and yaw rate versus time. This involves proportional control of the surge velocity, pitch rate and yaw rate variables within the model and generation of a reference input to describe the desired time histories for these variables. Output limiting is incorporated but rate limiting is not applied. In the first and third cases the manoeuvres do not take input variables to their maximum values while the second case involves a more demanding manoeuvre in which propeller speed and stern-plane deflection variables transiently reach their output limits.

4.1 A case involving specified patterns of surge velocity and pitch rate while the yaw rate is maintained at zero.

The detailed requirements in the example considered here involve finding the propeller and stern-plane inputs needed to produce a pattern of surge velocity involving an initial constant surge velocity of 5 m/s followed by a ramp-like change of surge-velocity of- 0.01 m/s^2 starting at time t = 20 s, together with an initial pitch-rate of zero followed by a constant pitch-rate of -0.01 rad/s from time t = 50 s. The yaw rate is maintained at a required value of zero throughout. In this case initial conditions of state variables within the vehicle model match the required values of surge velocity, pitch rate and yaw rate.

The gain factors of the proportional feedback loops were 100,000 for the loop involving the surge-velocity and 100 for the loops involving the pitch-rate and yaw-rate variables. These gain factors were found from analysis based on a linearised version of the model and through the use of simple trial and error methods involving the nonlinear simulation. A hard limit of 1500 revolutions per minute (rpm) was also placed on the permitted propeller speed and limits of ±20° in terms of the stern-plane and rudder actuator deflections. As can be seen from the results in Figs. 2a and 2b, the feedback loop is stable and shows no unsatisfactory transient behaviour for these gains. The requirements for both the variables shown are satisfied and both the propeller speed and stern-plane time histories make sense in simple physical terms for the required manoeuvre. Some coupling is present between the controls, as can be seen from the small step that occurs in the propeller speed at the time t = 50 s in Fig. 2b, when the stern-plane input is applied.

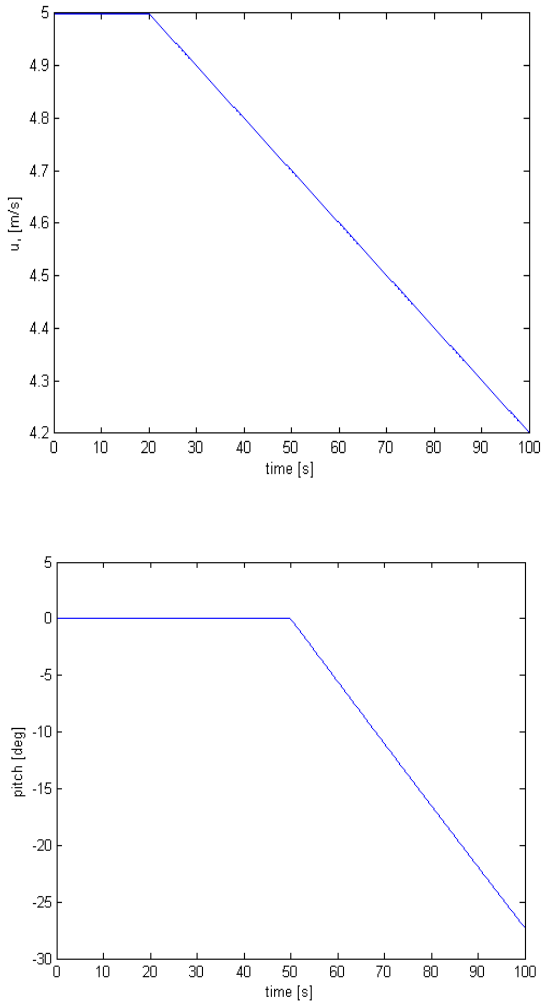

Fig.2a. Plots showing required patterns of surge velocity (Fig. 2a (i) - upper plot) and pitch angle (Fig 2a (ii) - lower plot) for the inverse simulation. In this case the inverse simulation has three feedback loops involving surge-velocity, pitch-rate and yaw-rate variables. The horizontal axis shows the time (s).

Although not included in the graphical results of Figs. 2a and 2b, the yaw rate was found to be very close to zero, leading to values of yaw angle which were smaller than 0.001 degree over the period of the manoeuvre. Coupling effects in terms of roll angle were also found to be very small (again with maxima less than 0.001 degree). As would be expected physically, the vertical velocity, *w*, was found to be influenced by the pitch change occurring at time t = 50 s.

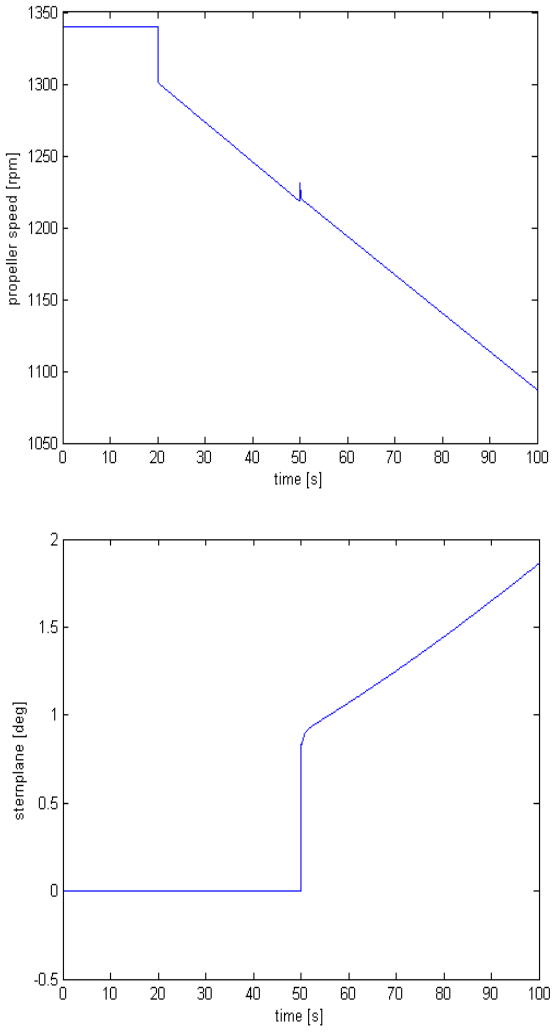

Fig. 2b. Plots showing the time histories of propeller speed in rpm (Fig. 2b (i) - upper plot) and stern-plane deflection in degrees (Fig. 2b (ii) - lower plot) that produce the patterns of surge velocity and pitch angle shown in Fig. 2a, as found by inverse simulation using three feedback loops involving surge-velocity, pitch-rate and yaw-rate variables. In both plots the horizontal axis shows the time (s). These results were obtained, as in the other cases considered, using a fixed-step Runge-Kutta integration method with integration step time of 0.01 s and communication interval of 0.1 s.

Although larger values of gain factor could be used, there is a tendency for numerical instability to arise in the surge-velocity loop when values much in excess of the chosen figure are used. Limit cycle behaviour may also be observed in the pitch-rate and yaw-rate loops for gains of 1000 or more. Smaller values of integration step size can be employed to overcome the numerical instability, but this is at the cost of increased execution time. As would be expected in a feedback system involving proportional control, the effect of reducing the loop-gain factors is to increase the error in the controlled variables.

4.2 The case of a manoeuvre which requires the propeller speed to reach its limiting value.

Fig. 3 shows results for the second case which involves changes in both the surge velocity and the pitch rate variables but with the yaw rate remaining constant, as in the previous case. However, in this example the initial surge velocity is only 3.88 m/s and this gives rise to an initial transient which causes the propeller speed to reach its limiting value of 1500 rpm.

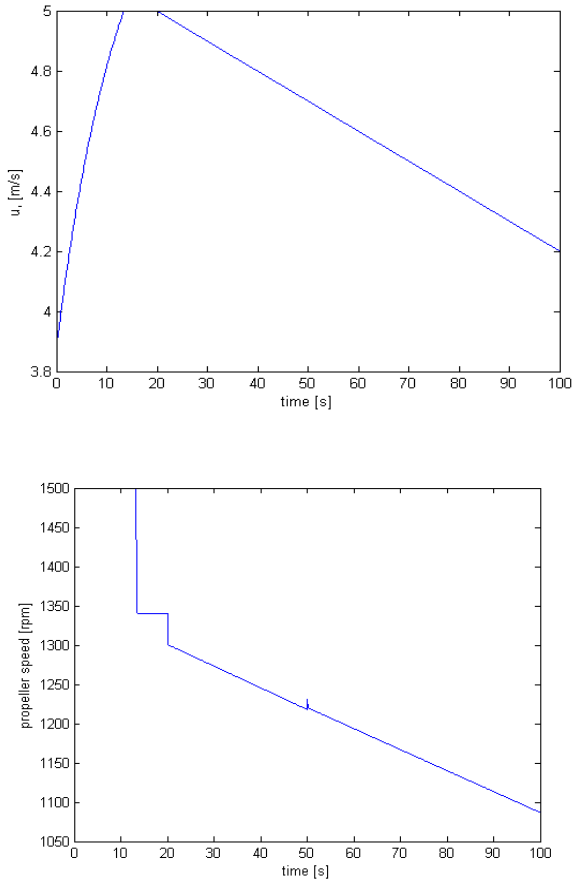

Fig. 3. Results for the case involving an initial condition in terms of surge velocity which gives rise to a propeller speed transient which reaches the limiting value of 1500 rpm. Fig. 3 (i) (the upper plot) shows the surge velocity (m/s) while Fig. 3 (ii) (the lower plot) shows the propeller speed (rpm). In both plots the horizontal axis shows the time (s).

Applying the propeller speed input found from the inverse simulation (lower plot in Fig. 3) to the forward model it is seen that the surge velocity (as shown in the upper plot of Fig. 3) increases rapidly over the first 12 s towards the required value of 5.0 m/s. During that initial period the propeller speed is at its limiting value, but when the surge velocity reaches the desired value of 5 m/s the propeller speed drops to a value of about 1340 rpm. This corresponds, as may be seen from Figure 2b, to the initial propeller speed in the first case considered. The results thus show very precisely the situations when propeller speed limiting occurs. Similar results have been obtained for cases involving limiting of other system inputs, such as those involving the rudder or stern-plane actuators. This provides important information which could be of value for design decisions in relation to the size of control surfaces and the required propulsive force.

From this result it is clear that, although the simple linear analysis of Section 2 does not apply in the nonlinear case, additional problems do not necessarily arise with the feedback system approach to inverse simulation when input variables, reach their maximum values. This supports similar findings in other studies and is important in terms of system design for manoeuvrability. It is believed that the ability to handle amplitude limits in a straightforward fashion is a potential advantage for the feedback approach compared with more conventional iterative methods of inverse simulation.

4.3 Case involving a specified time history for the yaw rate variable together with constant surge velocity and zero pitch-rate variables.

This case involves a lateral-directional manoeuvre in which there is an initial demanded yaw rate of zero, followed at time t = 50 s by the application of a constant required yaw rate of 0.01 rad/s. The required surge velocity is 3.88 m/s. and the required pitch rate is zero throughout. The rudder input found from the inverse simulation is displayed in Fig. 4 (i) (the upper plot of Fig. 4) and this shows a distinctive transient, involving a large overshoot in terms of the rudder deflection immediately following the demanded change of yaw rate.

The inverse simulation results also show that, in order to maintain the specified constant surge velocity and zero pitch rate, there is some coupling to the propeller and stern-plane inputs when the lateral-directional manoeuvre begins at time t = 50 s. As shown in Fig. 4 (ii) (the lower plot of Fig. 4), the change in steady-state propeller speed is of the order of 0.4%. Although not shown here in graphical form, the change in stern-plane deflection over the 50 second period of the manoeuvre was found to be less than 0.02 degree.

When the inputs found from the inverse simulation were applied to the forward model the simulation results were found to show a steady-state value of pitch rate which is very close to zero, together with a short transient in the pitch rate following the application of the demanded change of yaw rate. This pitch-rate transient had a peak magnitude which was of the order of 0.06 deg/s. Similarly, the forward simulation results showed a very short surge velocity transient, but no detectable steady-state change in surge velocity after the start of the lateral manoeuvre. In general, the magnitudes of errors such as these for the three constrained variables depend on the design of the feedback loops.

Coupling to other state variables were detected in the results, but these effects were found to be small in the case of the specific manoeuvre being considered. For example, following the rudder deflection a lateral velocity $v(t)$ of 0.035 m/s was introduced, together with a roll angle change of 0.6 degree (maximum). These coupling effects observed between the constrained variables and other state variables of the forward simulation model are associated with inherent coupling within the model of the UUV.

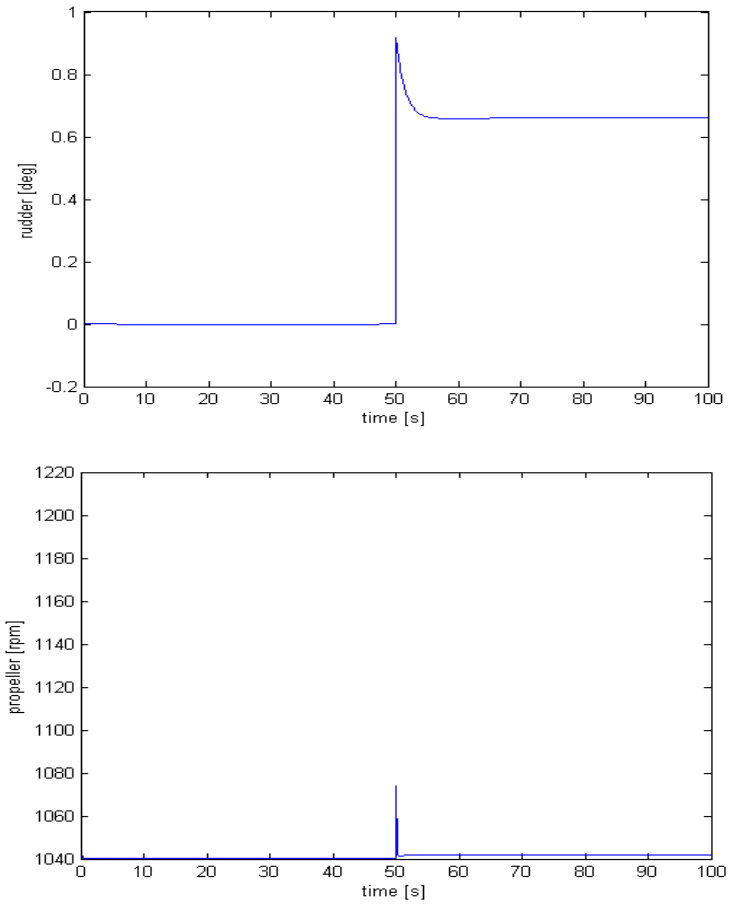

.

Fig. 4. The upper plot (Fig. 4 (i)) shows the rudder deflection (deg) while the lower plot (Fig. 4 (ii)) shows the propeller speed (rpm) found from inverse simulation for the case involving a demanded yaw-rate change. The horizontal axis shows the time (s). These results were obtained using a fixed-step Runge-Kutta integration method with integration step time of 0.01 s and communication interval of 0.1 s, as in the previous cases.

5. Inverse simulation of the nonlinear model for more complex manoeuvres.

For marine vehicles such as surface ships, the precisely defined manoeuvres that are traditionally performed to evaluate the performance, robustness and limitations of heading and steering control systems include the zig-zag manoeuvre, the turning circle manoeuvre and spiral manoeuvre [23]. As well as evaluating the steering, stability and stopping characteristics of the vessel under test, such manoeuvres may also be of value in providing

data from which quantitative estimates of ship model parameters may be found. Although similar tests could readily be carried out for an underwater vehicle such as the UUV being considered in this investigation, it is believed that manoeuvrability of a vehicle of this type can best be investigated through tests of the kind that have been developed for helicopter handling qualities and agility studies. Thomson and Bradley [3], include discussion concerning the mathematical modelling of manoeuvres based on an output vector consisting of predetermined flight-path coordinates and attitude angles represented as functions of time. The precise details of the manoeuvre depend on the intended application and two simple examples are the pop-up manoeuvre (used in low-level flight involving longitudinal controls to simulate avoidance of an obstacle) and the side-step manoeuvre (again used in low-level flight to avoid an obstacle, but this time by the use of lateral and directional controls). The slalom manoeuvre is a more complex case but is, once again, a task dominated by lateral and directional control inputs. The quick-hop provides another example and this involves acceleration of the vehicle to move it in a straight line from some specified initial condition in terms of position and velocity to some new position and velocity in a specified time. Manoeuvres of this kind can also be applied readily to underwater vehicles which have many characteristics that are similar in principle to those of helicopters and other forms of rotorcraft. It is believed that, for handling qualities and control investigations, such manoeuvres may provide more useful information for a UUV than the traditional tests applied to surface vessels since they can be used for all three of the vehicle axes.

The basic form of manoeuvre discussed by Thomson and Bradley [3] is based on a polynomial type of representation which can be written, in terms of positional variables, in the form:

$$p(t) = \left[6\left(\frac{t}{T_m}\right)^5 - 15\left(\frac{t}{T_m}\right)^4 + 10\left(\frac{t}{T_m}\right)^3\right]h \tag{17}$$

where T_m is the time taken to complete the manoeuvre and $p(t)$ is a position variable expressed in terms of the inertial reference frame. The quantity h determines the displacement from the original line of motion of the vehicle (e.g. lateral displacement in the case of a side-step or vertical displacement in the case of a pop-up manoeuvre). By differentiation it follows that the corresponding expressions in terms of velocity variables involve a similar polynomial form:

$$q(t) = \left[30\left(\frac{t}{T_m}\right)^4 - 60\left(\frac{t}{T_m}\right)^3 + 30\left(\frac{t}{T_m}\right)^2\right]\frac{h}{T_m} \tag{18}$$

Thomson and Bradley [3] suggest that, in the helicopter application, a fifth order polynomial of the form of Equation (17) provides adequate properties in terms of smoothness at the entry and exit points of the manoeuvre. The use of polynomial function provides a very simple solution to the modelling of flight paths and this form of function has also been used for the investigations of a number of manoeuvres using the UUV model.

Although Thomson and Bradley (e.g. [2], [3] and [26]) have worked mostly with trajectories defined in terms of inertial variables such as x_e, y_e and z_e, other researchers have also made use of attitude displacements as prescribed output variables (e.g. Hess, Gao and Wang [1]; Kato and Suguira [7]; Borri et al. [27]) and this latter approach has been

adopted in the current work but with profiles defined in terms of the polynomial type of representation of Equations (17) and (18). Several different types of manoeuvre have been considered and all involve use of this polynomial representation.

5.1 Case involving a pop-up type of manoeuvre.

In the case of the pop-up type of manoeuvre the inverse simulation involves feedback loops for surge velocity, heading and pitch attitude. In the case considered the required surge velocity is defined as a constant value (2.0 m/s) and the required heading is also held constant (at zero degrees). The time for the manoeuvre (T_m) is 40 s. A desired pitch change of the form given by Equation (18) is defined, with the factor h chosen to give a maximum pitch change (at time $T_m/2$) of 30 deg. Fig. 5 shows the results, with a maximum stern-plane deflection of approximately 12 deg producing the required form of pitch change. It can be seen that the surge velocity, u, remains close to the desired value and, although not shown in Fig. 5, the heading change is negligible, as required. The displacements x_e, y_e and z_e (defined in the Earth-fixed axis system) are as expected, with the longitudinal displacement consistent with the applied surge velocity (u), negligible lateral displacement y_e (as would be expected from the required zero value of heading change) and a maximum vertical displacement z_e of the order of 20m. The lateral (v) and vertical (w) velocity components are small, as required for this manoeuvre. Repeating the tests for other values of maximum pitch angle leads to results which show that the vertical distance moved increases in an approximately linear fashion until the pitch angle maximum reaches 50 deg when the stern-plane deflection approaches its limit of 20 deg.

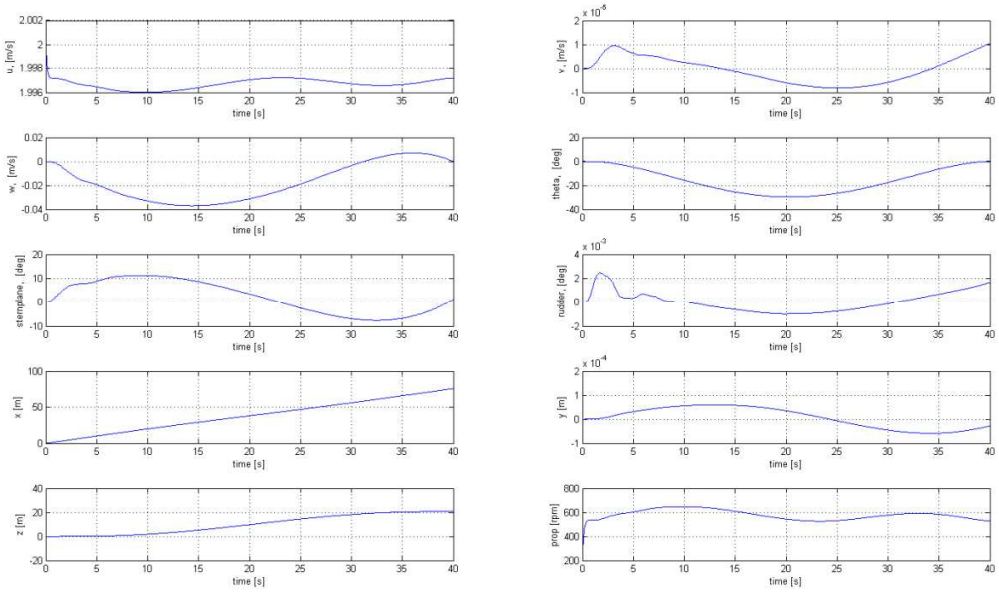

Fig. 5. Results found from inverse simulation with three feedback loops involving surge velocity, u (ms^{-1}, gain factor of 10^5), heading angle ψ (rad, gain factor 10) and pitch angle θ (rad, gain factor 100) variables. Simple proportional control was applied in each feedback loop and the reference inputs for speed and heading were constant. The reference input for the pitch feedback loop involved an expression of the form given in Equation (18) with a required maximum pitch change of 30 deg in the case shown here. The required surge velocity was constant at 2.0 ms^{-1} and the required heading was constant at 0 rad.

Fig. 6 presents the results for a demanded maximum pitch change of 60 deg for the same 40 s time interval and this shows very clearly that the stern-plane amplitude limit of 20 deg is reached at a time about six seconds from the start of the manoeuvre and the stern plane remains at its limit for a further period of about ten seconds. The pitch angle response is exactly as desired but additional results for other demanded pitch angle values show that the relationship between the maximum vertical displacement and maximum defined pitch angle has become nonlinear. Hence, under conditions where limiting occurs, definition of the trajectory in terms of pitch attitude does not allow the maximum vertical displacement of the vehicle to be predicted as easily as in the situation without limiting.

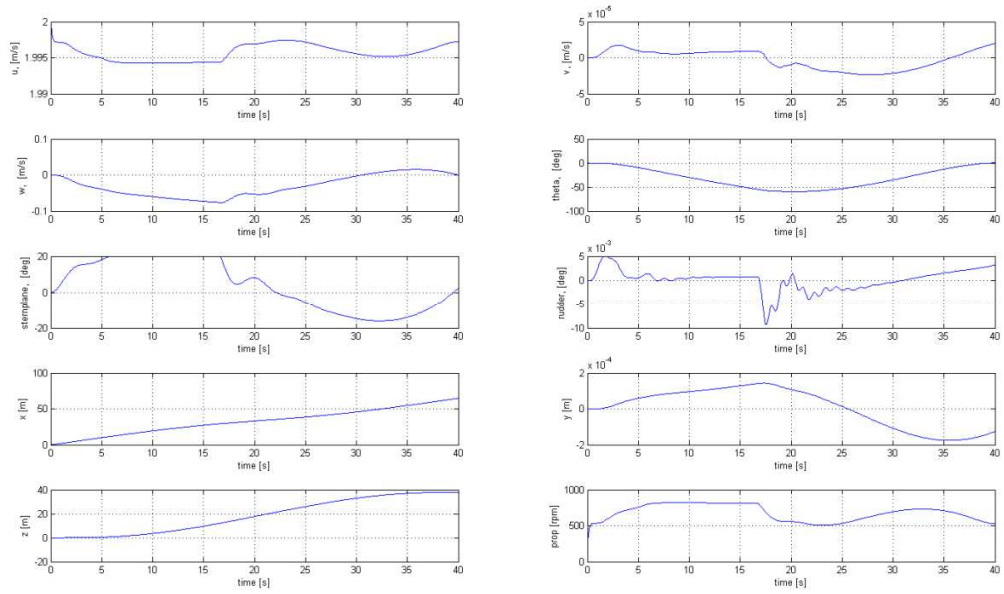

Fig.6. Results which indicate stern-plane limiting found from inverse simulation for the same situation as in the case of the results of Fig. 5 but with a demanded maximum pitch change of 60 deg.

5.2 Case involving a side-step type of manoeuvre.

The side-step manoeuvre again involves three loops with, in this case, surge velocity, heading and pitch attitude as the feedback variables. In the specific example considered the required surge velocity is defined as a constant value (3.0 m/s for the first case considered) and the required pitch attitude is also required to be held constant (at zero degrees). The time for the manoeuvre (T_m) is chosen to be 40 s. A desired heading change of the form given by Equation (18) is defined, with the factor h chosen to give a maximum heading change (at time $T_m/2$) of -30 deg. Fig. 7 shows the results, with a maximum rudder deflection of approximately 4 deg producing the required form of heading angle change with a maximum of -30 deg, as demanded from the given reference input. The results show that other variables, such as the surge velocity (u), remain close to the required values. Examination of the displacements x_e, y_e and z_e (defined in the Earth-fixed axis system) show that the longitudinal displacement (x) is, once again, consistent with the applied surge velocity and that there is a maximum lateral displacement (y) of the order of 32.5 m,

with negligible vertical displacement (z). As in the previous case, repetition of the tests for other values of maximum heading angle altered the lateral displacement y_e in an approximately linear fashion. Thus definition of the maximum heading change effectively defines the maximum lateral displacement y_e.

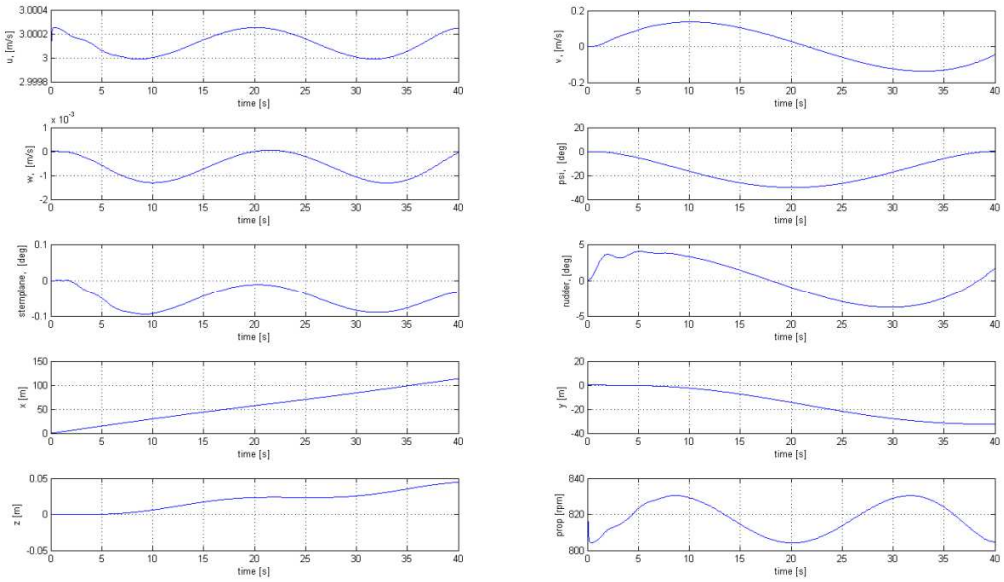

Fig. 7. Inverse simulation for the case involving a demanded change of heading angle with a maximum heading (ψ (psi)) of -30 deg at time t=20 s and a required constant surge velocity (u) of 3.0 ms^{-1}. The vertical velocity (w) is very small while the lateral velocity (v) is consistent with the form of manoeuvre demanded. The forward displacement (x) is consistent with the required surge velocity and the lateral displacement (y) is consistent with the requirements, while the vertical displacement (z) remains small throughout. The feedback variables in this case were surge velocity, u (ms^{-1}, gain factor of 10^5), heading angle ψ (rad, gain factor 10) and pitch angle θ (rad, gain factor 100).

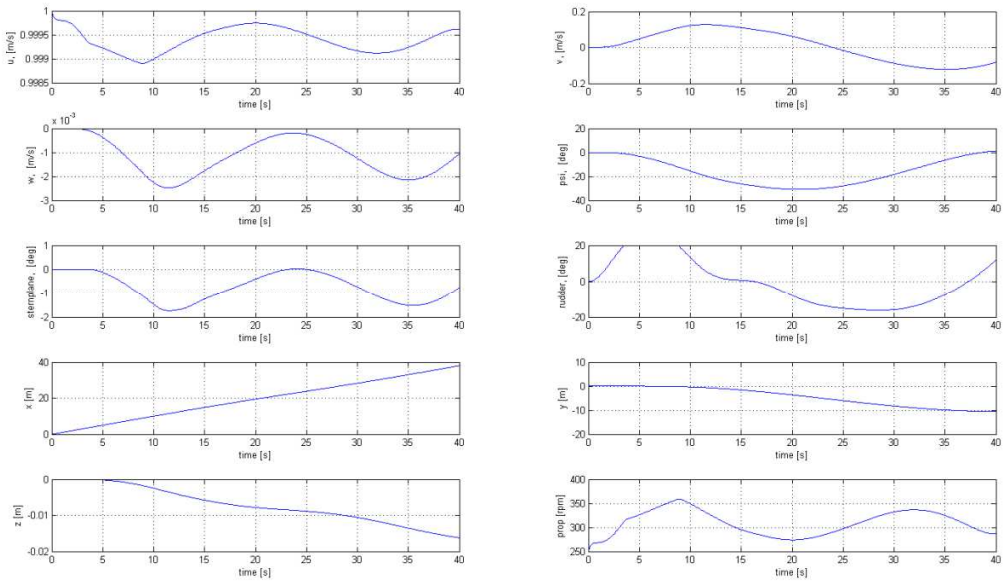

Fig. 8. Inverse simulation for a case similar to that of Fig. 7, but with a forward speed (surge velocity) of 1.0 ms^{-1} , showing limiting of the rudder at +20 deg. The feedback loop gains in this case were as specified for Fig. 7.

The effectiveness of the rudder in producing heading changes depends on the surge velocity of the vehicle and it has been found that if the required surge velocity value is decreased to 1.0 m/s the rudder reaches its limit of 20 deg. The results, shown in Fig. 8, indicate clearly that there are interactions between the rudder and propeller feedback loops and that the action of the propeller changes during the period when the rudder is at its limit. The inverse simulation approach based on feedback does, however, continue to provide the required inverse solution and also offers useful physical insight when limiting action occurs.

5.3 Case involving a quick-hop type of manoeuvre.

The third case considered involving a more complex manoeuvre involved a quick-hop situation in which the vehicle is required to accelerate smoothly from a given initial surge velocity to a defined maximum and then decelerate smoothly back to the initial speed in a defined time (T_m). This case involves feedback loops for surge velocity, heading and pitch attitude. The required initial surge velocity was defined as a constant value (1.0 m/s) and a surge velocity change of the form given by Equation (18) was defined, to give a maximum surge velocity change (at time $T_m/2$) of 1.1m/s. The feedback variables in this case were surge velocity, u (ms^{-1}, gain factor of 10^5), heading angle ψ (rad, gain factor 10) and pitch angle θ (rad, gain factor 100). The heading and pitch angle feedback loops involved constant reference inputs of zero. Fig. 9 shows results for this modified value of surge velocity loop gain, indicating a maximum propeller speed change of approximately 700 rpm, in order to produce the form of surge velocity change demanded from the given reference input. It can be seen that other constrained variables remain close to the required

reference values and the displacements x_e, y_e and z_e (defined in the Earth-fixed axis system) are consistent.

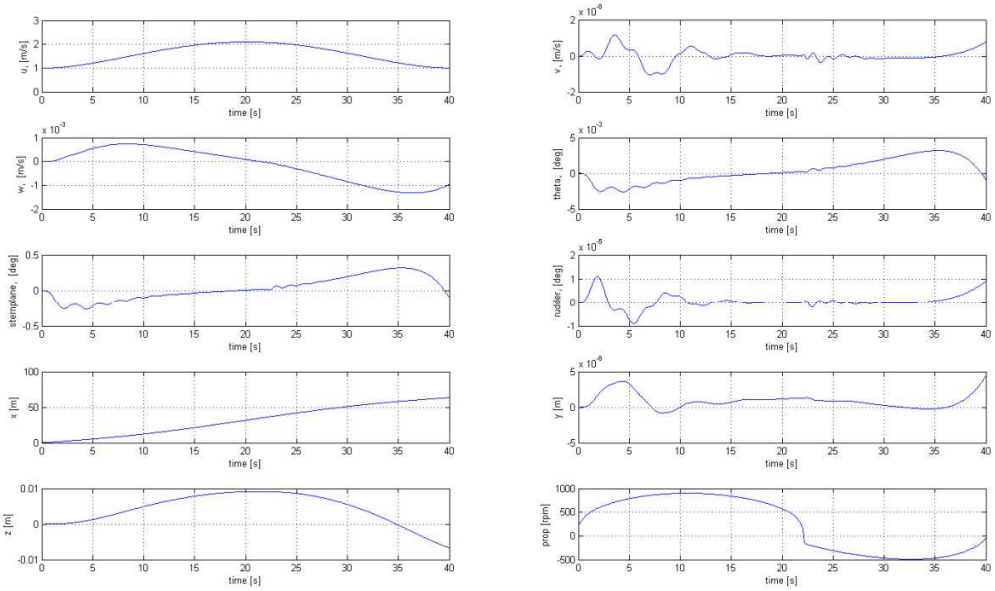

Fig. 9. Inverse simulation results for the quick-hop manoeuvre for a defined surge velocity change (u). The feedback loop gain for the surge velocity feedback loop was 10^5 in this case with heading angle loop gain factor of 10 and pitch angle loop gain factor of 100. Other variables shown here are as defined previously

6. Discussion and Conclusions

The inverse simulation results presented above are encouraging, both for the examples involving output responses of simple form and the cases involving more complex manoeuvres such as the pop-up, side-step and quick-hop. With feedback loops based on proportional control, steady–state errors do exist (as would be expected) but these errors are generally predictable and, through appropriate choices of gain factors, we can ensure that these errors are of very small magnitude. In principle, errors could be further reduced by the introduction of more complex forms of feedback involving a combination of output feedback and output rate feedback (or some other form of state-variable feedback). However, application of the time histories found from inverse simulation to the corresponding forward models shows that, for this application, the levels of accuracy achieved with simple proportional control are acceptable and more complex forms of feedback structure are not required.

There are six inputs and twelve possible outputs for the UUV model and decisions have to be made by the investigator about which actuators should be associated with each output variable in forming the feedback loops for the inverse simulations. This was possible through simple physical reasoning in the case considered and no difficulties were encountered. However, issues of input-output pairing could be a topic for further investigation for other applications.

Insight obtained from the inverse simulation results could have an important bearing on design issues for an underwater vehicle of this kind, especially in terms of the installed power, battery capacity and the characteristics of the propeller, actuator and control surfaces in relation to the intended role of the vehicle. Inverse simulation results show very clearly whether or not the vehicle can perform a specified manoeuvre and, in cases where the manoeuvre is possible, the results indicate directly how close the system is to the limits on propeller speed and actuator deflection. Interactions between the control inputs required to perform a specified manoeuvre also show up very clearly from the inverse simulation results. More complex models of actuators could easily be included in inverse simulation studies of this kind and these could incorporate rate limits and other dynamic effects such as dead-zone, in addition to the amplitude limiting effects considered in this investigation.

The closed-loop system inevitably has a longer execution time for simulation than the forward model because the integration interval, generally, has to be shorter. It has been found that investigations based on linearised descriptions can provide useful insight regarding the optimum choice of integration step size and integration method for this type of approach.

One very important point about the feedback approach is that the problem of designing a feedback system for an inverse model is, in general terms, significantly less difficult than that of designing a feedback system for a control system application involving a model of similar complexity. Questions of response to external disturbances, insensitivity to measurement noise and robustness in terms of model uncertainties are all irrelevant in the inverse simulation case since disturbances and measurement noise are not present. The model is also completely known so there are no issues of robustness (other than numerical robustness). There may well be uncertainties within the model when compared with the corresponding real system but, for the purposes of inverting a given model, no uncertainty exists. Relatively simple methods of feedback system design involving high-gain solutions and state-variable feedback can therefore be considered for the model inversion application. Although problems of numerical stiffness can arise with the feedback approach to inverse simulation this need not create major difficulties, for most applications, if an appropriate choice of numerical integration algorithm is made.

In conclusion, this application involving the UUV model has shown that inverse simulation methods provide insight for engineering investigations that is different from the understanding that comes from conventional modelling and simulation studies. Viewing the system in terms of the inputs that are needed to achieve a defined pattern of outputs provides the investigator with information that is directly relevant for engineering design, especially in the context of actuators. It is believed that this understanding could not be obtained so readily using traditional modelling and simulation methods. It is also believed that this application provides further evidence of the value of the feedback approach to inverse simulation. It therefore provides an important alternative to the other numerical and iterative methods of inverse simulation mentioned in Section 1 (Introduction).

ACKNOWLEDGEMENTS

The author wishes to thank the US Office of Naval Research for the funding that supports the work described in this paper through awards to California State University, Chico and associated sub-contracts placed at the University of Glasgow by California State University, Chico. The author also wishes to thank Dr R.E. Crosbie of the Department of Electrical and Computer Engineering, California State University, Chico, for the support and continuing interest that he has shown in this research.

REFERENCES

[1] R.A. Hess, C. Gao. and S.H. Wang, A generalized technique for inverse simulation applied to aircraft maneuvers. *AIAA J. Guidance Control and Dynamics*, 14 (5) (1991), pp. 920-926.
[2] D.G. Thomson and R. Bradley, The principles and practical application of helicopter inverse simulation, *Simulation Practice and Theory*, 6 (1) (1998), pp. 47-70.
[3] D. Thomson and R. Bradley, Inverse simulation as a tool for flight dynamics research - principles and applications, *Progress in Aerospace Sciences*, 42 (3) (2006), pp.174-210.
[4] L.Lu, D.J. Murray-Smith and D.G. Thomson, Issues of numerical accuracy and stability in inverse simulation, *Simulation Modelling Practice and Theory*, 16 (2008), pp. 1350-1364.
[5] S. Rutherford and D.G. Thomson, Improved methodology for inverse simulation, *Aeronautical Journal*, 100 (993) (1996), pp. 79-86.
[6] D. Anderson, Modification of a generalised inverse simulation technique for rotorcraft flight, *Proc. Inst. Mech. Eng.*, (*Part G – J. Aerospace Eng.*), 217 (2003), pp. 61-73.
[7] O. Kato and I. Suguira, An interpretation of airplane motion and control as inverse problems, *AIAA J. Guidance, Control and Dynamics*, 9 (2) (1986), 198-204.
[8] S. Lee and Y. Kim, Time domain finite element method for inverse problem of aircraft maneuvers, *AIAA J. Guidance, Control and Dynamics*,20 (1) (1997), pp. 97-103.
[9] R. Celi, Optimisation based inverse simulation of a helicopter slalom maneuver, *AIAA J. Guidance Control and Dynamics*, 23 (2), (2000), pp. 289-297.
[10] M. Thümme, G Looye, M. Kurze, M. Otter and J. Bals , *Nonlinear inverse models for control*, In (Ed.: G. Schmitz), Proceedings of the 4th International Modelica Conference, Hamburg, Germany, March 7-8, 2005, pp. 267-279, Modelica Organisation, Linköping, Sweden, 2005.
[11] D.J. Murray-Smith, *Modelling and Simulation of Integrated Systems in Engineering*, Chapter 4, Woodhead Publishing, Cambridge, UK, 2012.
[12] M. Fleiss, J. Lévine, P. Martin and P. Rouchon, Flatness and defect of non-linear systems: introductory theory and examples, *International J. Control*, 61 (6), 1995, pp. 1327-1361.
[13] W. Blajer and K. Kołodziejczky, Improved DAE formulation for inverse dynamics simulation of cranes, *Multibody System Dynamics*, 25 (2), 2011, pp. 131-143.
[14] G. Irwin, K. Warwick and K.J. Hunt, (eds.), *Neural Network Applications in Control*, pp. 125-128, Institution of Electrical Engineers, Stevenage, UK, 1995.
[15] J.J. Buchholz and W. von Grünhagen, *Inversion Impossible?*, Technical Report, University of Applied Sciences Bremen, Germany, September 2004.
[16] Y.Tagawa and K. Fukui, *Inverse dynamics calculation of nonlinear model using low sensitivity compensator*. In, Proceedings of Dynamics and Design Conference, 1994, pp. 185-188.
[17] G. Venture, T. Kojima and Y. Tagawa, *Fast motion control of robotic systems using inverse dynamics compensation via 'simulation of feedback control systems' (IDCS)*. In, Proceedings of 1st Joint Conference on Multibody System Dynamics, May 25-27 2010, Lapeenranta, Finland.
[18] Y. Tagawa, J.-Y. Tu and D.P. Stoten, Inverse dynamics compensation via 'simulation of feedback control systems', *Proceedings Institution of Mechanical Engineers, Part I: J. Systems and Control Engineering*, 225 (2012), 137-153.

[19] D.J. Murray-Smith, Feedback methods for inverse simulation of dynamic models for engineering applications, *Mathematical and Computer Modelling of Dynamical Systems*, 17 (5) (2011), pp. 515-541.
[20] D.J. Murray-Smith, The application of parameter sensitivity analysis methods to inverse simulation models, *Mathematical and Computer Modelling of Dynamical Systems*, 19 (1) (2013), pp. 67-90.
[21] A.J. Healey and D. Lienard, Multivariable sliding mode control for autonomous diving and steering of unmanned underwater vehicles, *IEEE Journal of Oceanic Engineering*, 18 (3) (1993), pp. 327-339.
[22] J.J. Zenor, D.J. Murray-Smith, E.W. McGookin and R.E. Crosbie, Development of a multi-rate simulation model of an unmanned underwater vehicle. In Troch, I. and Breitenecker, F., (eds), *Proceedings Mathmod Conference, Vienna, 2009*, pp. 1950-1957, Argesim, Vienna, Austria, 2009.
[23] T.I. Fossen , *Guidance and Control of Ocean Vehicles*, Wiley, Chichester, UK, 1994.
[24] S.F. Hoerner, *Fluid Dynamic Drag*, Hoerner Publications, New York, USA, 1968.
[25] MSS, Marine Systems Simulator (2010).
[Online] http://www.marinecontrol.org (Accessed 16.12.2012).
[26] D. G. Thomson and R. Bradley, Mathematical definition of helicopter maneuvers, *J. American Helicopter Society*, 42 (4) (1997), 307-309.
[27] M. Borri, C.L. Bottasso and F. Montelaghi, Numerical approach to inverse flight dynamics, *AIAA J. Guidance Control and Dynamics*, 20 (4) (1997), 742-747.